

Spectral correlations in Anderson insulating wires

M. Marinho and T. Micklitz

Centro Brasileiro de Pesquisas Físicas, Rua Xavier Sigaud 150, 22290-180, Rio de Janeiro, Brazil

(Dated: July 3, 2021)

We calculate the spectral level-level correlation function of Anderson insulating wires for all three Wigner-Dyson classes. A measurement of its Fourier transform, the spectral form factor, is within reach of state-of-the-art cold atom quantum quench experiments, and we find good agreement with recent numerical simulations of the latter. Our derivation builds on a representation of the level-level correlation function in terms of a local generating function which may prove useful in other contexts.

PACS numbers: 72.15.Rn, 73.20.Fz, 03.75.-b, 42.25.Dd

Introduction:—Localization due to quantum interference in disordered systems [1] is one of the cornerstones of condensed matter physics, with exciting recent developments such as topological Anderson insulators [2–6] and many-body localization [7, 8]. Notwithstanding our profound understanding of the single-particle localization problem, examples of dynamical correlation functions within the Anderson insulating phase, which are accessible to direct experimental verification, are rare. The experimental challenge is to provide set-ups which allow for the controlled observation of strong localization via some tunable parameter [9]. On theoretical side one faces the notorious difficulty that Anderson insulators reside in the non-perturbative strong coupling limit of a nonlinear field theory [10].

A series of recent papers proposes the direct observation of spectral correlations in Anderson insulators within a cold atom quantum quench experiment [11–14]. A specifically promising variant of this proposal builds on a cold atom realization of the kicked rotor and is within reach of state-of-the-art experiments [15]. The quench protocol is summarized as follows: (i) A cloud of cold atoms is prepared in an initial state with a well-defined momentum \mathbf{k}_i , (ii) it is let to propagate freely under the influence of a disorder potential for some time t , at which (iii) the disorder is turned off and the atomic momentum distribution $\rho(\mathbf{k}_f, t)$ is measured. A forward scattering peak at $\mathbf{k}_f \simeq \mathbf{k}_i$ is predicted to appear as a manifestation of an accumulation of those quantum coherence processes leading to strong Anderson localization. Within the quench set-up ‘time’ plays the role of the control parameter and the genesis of the forward scattering peak is described by the spectral form factor. The latter is the Fourier transform of the connected level-level correlation function,

$$K(\omega, L) = \nu_0^{-2} \langle \nu(\epsilon + \frac{\omega}{2}) \nu(\epsilon - \frac{\omega}{2}) \rangle_c, \quad (1)$$

where ν_0 is the density of states (per spin) at the energy shell.

The theoretical study of level-level correlations (1) in disordered systems has a long history [16–25]. Analytical results are, however, only known in specific limits. In

low-dimensional systems ($d < 3$) Eq. (1) describes how Wigner-Dyson statistics at small system sizes L evolves into Poisson statistics with increasing size. The former is associated with non-integrable chaotic dynamics, while the latter signals the breaking of ergodicity due to quantum localization [26, 27]. Fully uncorrelated Poisson statistics only realizes in the thermodynamic limit of unbounded system sizes, and spectral correlations remain in finite size systems. It is these correlations which are accessible in the cold atom quench experiment, however, only asymptotic results are known for the experimentally relevant orthogonal and the symplectic symmetry class.

In this paper we derive the spectral level-level correlation function for Anderson insulating wires belonging to the three Wigner-Dyson classes. We show that the latter is readily calculated from the ground-state wavefunction of the transfermatrix Hamiltonian for the supersymmetric σ -model reported in Ref. [28]. Our results are in perfect agreement with recent numerical simulations of the quench experiment [15], and their experimental verification would mark an important benchmark for our understanding of strong Anderson localization.

Field theory:—We start out from the field theory description of the level-level correlation function for a d -dimensional disordered system [10, 18, 29],

$$K(\omega) = \frac{1}{64} \text{Re} \langle [\int (dx) \text{str} (k\Lambda Q_\Lambda)]^2 \rangle_S. \quad (2)$$

Here the average, $\langle \dots \rangle_S \equiv \int \mathcal{D}Q(\dots) \exp(S)$, is with respect to the diffusive nonlinear σ -model action,

$$S = -\frac{\pi\tilde{\nu}_0}{8} \int (dx) \text{str} (D(\partial_x Q)^2 + 2i\omega\Lambda Q), \quad (3)$$

with D the classical diffusion constant, ‘str’ the generalization of the matrix trace to ‘super’-space, and $\int (dx) = 1$. The system belongs to one of the three Wigner-Dyson symmetry classes, characterized by the absence of time-reversal symmetry, $\mathcal{T} = 0$ (unitary class), presence of time-reversal and spin-rotational symmetry, $\mathcal{T}^2 = 1$ (orthogonal class), or presence of time-reversal and absence of spin-rotational symmetry, $\mathcal{T}^2 = -1$ (symplectic class). Throughout the paper, we adopt

the notation of Ref. 10 where $\tilde{\nu}_0 = \nu_0$ in the unitary and orthogonal, and $\tilde{\nu}_0 = 2\nu_0$ in the symplectic class. Q is a supermatrix acting on an 8-dimensional graded space, which is the product of two-dimensional subspaces, referred to as ‘bosonic-fermionic’ (bf), ‘retarded-advanced’ (ra) and ‘time-reversal’ (tr) sectors. Matrices $k \equiv \sigma_3^{\text{bf}}$, $\Lambda \equiv \sigma_3^{\text{ra}}$ break symmetry in bosonic-fermionic and advanced-retarded sectors, respectively. Λ describes the classical, diffusive fixed point and $Q_\Lambda \equiv Q - \Lambda$ deviations from the latter. Drawing on the similarity of action (3) to Ginzburg-Landau theories for phase-transitions, ‘str(ΛQ)’ corresponds to a symmetry breaking term relevant at large level-separations or short time scales $t \sim \omega^{-1} \ll \Delta_\xi^{-1} \equiv \xi^2/D$, with ξ the localization length. In this diffusive limit $Q \simeq \Lambda$, which allows for a controlled perturbative expansion in Goldstone modes, viz., the diffusion modes of the disordered single-particle system. Strong Anderson localization sets in at $t \sim \omega^{-1} \sim \Delta_\xi^{-1}$ when large fluctuations restore the symmetry in the ‘ra’-sector. This requires integration over the entire Q -field manifold and calls for non-perturbative methods. Such methods are available for quasi one-dimensional geometries $L \gg L_\perp$, where the functional integral with action (3) takes the form of a path-integral of a quantum mechanical particle with coordinate Q and mass $\sim 1/D$, moving in a potential $\sim \text{str}(\Lambda Q)$. The latter can be mapped onto the corresponding Schrödinger problem, and we next follow this strategy.

Anderson insulating wires:—Concentrating then on a quasi one-dimensional geometry, one needs to express the spectral correlation function Eq. (2) in terms of eigenfunctions of the Hamiltonian for the Schrödinger problem, known as the ‘transfermatrix Hamiltonian’. This has been done in previous work [10, 30]. The resulting equations for the relevant functions are, however, rather complex and closed solutions for all Wigner-Dyson classes are unknown. We therefore follow here a different route, which employs the graded symmetry of action (3) in order to derive Eq. (1) from a local generating function. The latter depends only on the ground-state wave-function, i.e. ‘zero-modes’ of the transfermatrix Hamiltonian. This implies a significant simplification of the problem, and allows for an exact calculation of correlations (1). We momentarily postpone the discussion of the rather technical derivation, and state the final expression for the generating function in case of Anderson insulating wires $L \gg \xi \equiv \pi\tilde{\nu}_0 D/L$ [31],

$$\begin{aligned} K(\omega) &= \frac{\xi}{2\beta L} \text{Re} \int (dx) \partial_\eta \mathcal{F}(\eta, x)|_{\eta = -\frac{i\omega}{\Delta_\xi}}, \\ \mathcal{F}(\eta) &= \frac{1}{2} \int dQ_0 \text{str}(\Lambda Q_0) Y_0^2(Q_0). \end{aligned} \quad (4)$$

Here Y_0 is the ground-state wave-function of the Schrödinger problem detailed below, and we introduced the symmetry parameter $\beta = 1(2)$ in the orthogonal and symplectic (unitary) class. Notice that in Eq. (4)

we already integrated out some c -number and all Grassmann variables. That is, Q_0 here depends only on c -number variables from the compact interval, $-1 \leq \lambda_f \leq 1$ (‘fermionic radial variables’), and non-compact interval $1 \leq \lambda_b$ (‘bosonic radial variables’). The precise number of radial variables depends on the symmetry class i.e. $Q_0(\mathcal{R})$, with $\mathcal{R} = \{\lambda_f, \lambda_b\}$, $\{\lambda_f, \lambda_{b,1}, \lambda_{b,2}\}$, and $\{\lambda_{f,1}, \lambda_{f,2}, \lambda_b\}$, in the unitary, orthogonal and symplectic classes, respectively. Similarly, $dQ_0 = d\mathcal{R} \sqrt{g(\Lambda)}$, with Jacobians $\sqrt{g} = 1/(\lambda_b - \lambda_f)^2$, $\sqrt{g} = (1 - \lambda_f^2)/(\lambda_1^2 + \lambda_2^2 + \lambda_f^2 - 2\lambda_1\lambda_2\lambda_f - 1)^2$, and $\sqrt{g} = (\lambda_b^2 - 1)/(\lambda_1^2 + \lambda_2^2 + \lambda_b^2 - 2\lambda_1\lambda_2\lambda_b - 1)^2$ for the three symmetry classes, and $d\mathcal{R}$ the flat measure. For notational convenience we suppress the graded index b, f in favor of the ‘tr’-index 1, 2. The ground-state wave-function is a solution to the homogeneous equation,

$$(-\Delta_Q + \frac{\eta}{2} \text{str}(\Lambda Q_0)) Y_0(Q_0) = 0, \quad (5)$$

obeying the boundary condition $Y_0(\Lambda) = 1$ and we recall that at $Q_0 = \Lambda$ all radial coordinates $\lambda = 1$. Here we introduced $\eta = -i\omega/\Delta_\xi$, and $\Delta_Q = \frac{1}{\sqrt{g}} \partial_\lambda \sqrt{g} g^{\lambda\rho} \partial_\rho$ is the Beltrami-Laplace operator on the Q_0 -field manifold with repeated indices running over radial variables, $\lambda, \rho \in \mathcal{R}$ and metric tensor $g^{\lambda\rho} = |\lambda^2 - 1| \delta^{\lambda\rho}$ in all symmetry classes, with $\delta^{\lambda\rho}$ the Kronecker-delta.

Correlations from zero-mode:—We may then use the Schrödinger equation to express $\text{str}(\Lambda Q_0) Y_0 = -(2\Delta_Q + \eta \text{str}(\Lambda Q_0)) Y_0'$ and $\eta \text{str}(\Lambda Q_0) Y_0 = -2\Delta_Q Y_0$, and arrive at

$$\mathcal{F}(\eta) = \int dQ_0 (Y_0' \Delta_Q Y_0 - Y_0 \Delta_Q Y_0'), \quad (6)$$

where we introduced $Y_0' \equiv \partial_\eta Y_0$. Upon partial integration this results in the boundary contribution

$$\mathcal{F}(\eta) = \int d\mathcal{R} \partial_\lambda \sqrt{g} g^{\lambda\rho} (Y_0' \partial_\rho Y_0 - Y_0 \partial_\rho Y_0'). \quad (7)$$

At this point we notice that metric elements $g^{\lambda\rho}$ vanish at any boundary point $\lambda = 1$. At the same time, the Jacobian is singular at $Q_0 = \Lambda$ where all $\lambda_b, \lambda_f = 1$. To deal with this situation we regularize the integral Eq. (7) in any of the variables λ , shifting the bound of integration to $1^\pm \equiv 1 \pm \epsilon$ with \pm for a bosonic/fermionic variable. In the limit $\epsilon \searrow 0$ the boundary contribution $(\sqrt{g} g^{\lambda\rho})|_{\lambda=1^\pm}$ then reduces (up to a numerical factor) to a δ -function in the remaining radial coordinates, fixing $Q_0 = \Lambda$. Noting further that $Y_0(\Lambda) = 1$ and $Y_0'(\Lambda) = 0$, we arrive at the remarkably simple expression

$$\mathcal{F}(\eta) = -2\partial_{\lambda_f} Y_0'|_{Q=\Lambda}, \quad (8)$$

where in the symplectic class λ_f can be either $\lambda_{1,2}$. It can be verified that $\partial_\lambda Y_0'|_{Q=\Lambda} = \pm \partial_\rho Y_0'|_{Q=\Lambda}$, where the positive sign applies if λ and ρ are both bosonic or fermionic radial variables and the negative sign else. This guarantees that Eq. (8) does not depend on the regularization

scheme, and one may, e.g., symmetrize the result in the radial variables [32]. An equivalent relation between the ground-state wave-function and the generating function for spectral correlations has been previously encountered for the unitary class [33, 34]. In this case the derivation is built upon a mapping of the localization problem in the unitary class to the three-dimensional Coulomb-problem [35]. The above Eq. (8) shows that the simple relation is not accidental but applies to all Wigner-Dyson symmetry classes.

Using then the recent results of Ref. [28, 32] for the ground-state wave-functions we find ($z_\eta \equiv 4\sqrt{\eta}$)

$$\mathcal{F}^U(\eta) = -8I_0(z_\eta)K_0(z_\eta), \quad (9)$$

$$\mathcal{F}^O(\eta) = -4(I_0(z_\eta)K_0(z_\eta) + I_1(z_\eta)K_1(z_\eta)), \quad (10)$$

$$\mathcal{F}_\pm^{\text{Sp}}(\eta) = -4([I_0(z_\eta) \pm 1]K_0(z_\eta) + I_1(z_\eta)K_1(z_\eta)), \quad (11)$$

where ‘U’, ‘O’, and ‘Sp’ refers to the unitary, orthogonal and symplectic symmetry class, respectively, and ‘+/-’ indicates an even/odd number of channels.

Spectral correlations:—From Eqs. (9)-(11) we find the level-level correlations in Anderson insulating wires for all three Wigner-Dyson classes,

$$K(\omega) = \frac{32\xi}{\beta L} \text{Re} \mathcal{K}(z_\eta)|_{z_\eta=4\sqrt{-i\omega/\Delta\xi}}, \quad (12)$$

where

$$\mathcal{K}^U(z_\eta) = [K_1(z_\eta)I_0(z_\eta) - K_0(z_\eta)I_1(z_\eta)]/z_\eta, \quad (13)$$

$$\mathcal{K}^O(z_\eta) = K_1(z_\eta)I_1(z_\eta)/z_\eta^2, \quad (14)$$

$$\mathcal{K}_\pm^{\text{Sp}}(z_\eta) = K_1(z_\eta)[I_1(z_\eta) \pm z_\eta/2]/z_\eta^2. \quad (15)$$

Eqs. (12)-(15) are the main result of this paper. Strict Poisson statistics only applies for $\lim_{L \rightarrow \infty} K(L, \omega) = 0$, and correlations between localized eigenstates remain in any finite system. At large level-separation ($s \equiv \omega/\Delta\xi \gg 1$) these reflect the classically diffusive dynamics on short time-scales, on which quantum interference processes remain largely undeveloped. Correlations of close-by levels ($s \equiv \omega/\Delta\xi \lesssim 1$), on the other hand, store information on the long-time limit, i.e. the deep quantum regime in which remaining dynamical processes are due to tunneling between almost degenerate, far-distant localized states [36–38]. The crossover between these two limits, described by Eqs. (12)-(15), is shown in Fig 1. For a comparison with fully chaotic systems we also show in the inset the corresponding Wigner-Dyson correlations with their characteristic level repulsion at small level-separations, and contrasting the residual logarithmic level repulsion between localized states.

From the above expression, one readily recovers asymptotic correlations of far-distant levels $s \gg 1$, applying to all Wigner-Dyson classes [39],

$$\frac{L}{\xi} K(s) = -\frac{1}{4\sqrt{2}\beta} \left(\frac{1}{s^{3/2}} - \frac{(-1)^\beta 3}{128s^{5/2}} + \dots \right), \quad (16)$$

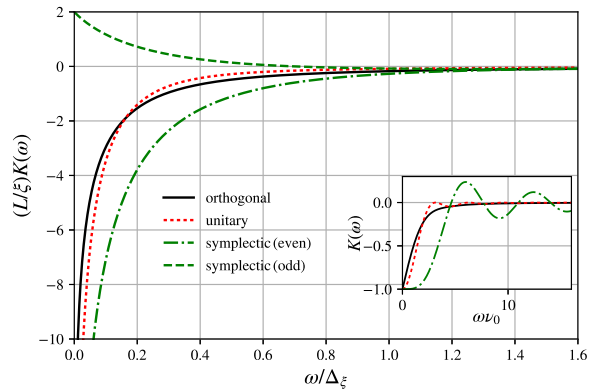


Figure 1: Level-level correlations in Anderson insulating wires for the Wigner-Dyson classes. The residual level-attraction in the symplectic class with an odd number of channels reflects the presence of a topologically protected metallic channel. The inset shows for comparison Wigner-Dyson spectral correlations of fully chaotic systems.

with the leading Altshuler-Shklovskii contribution [19, 40]. For small level-separations and systems in the unitary, orthogonal or symplectic class with an even number of channels ($s \ll 1$)

$$\frac{L}{\xi} K(s) = -a_\beta (\log(1/4s) - 2\gamma + b_\beta + c_\beta \pi s + \dots), \quad (17)$$

where $\gamma \simeq 0.577$ the Euler-Mascheroni constant, $a_{\text{U,Sp}+} = 8$, $a_{\text{O}} = 4$, $b_{\text{U}} = 0$, $b_{\text{O}} = 1/2$, $b_{\text{Sp}+} = 3/4$, and $c_{\text{U}} = 3$, $c_{\text{O}} = 2$, $c_{\text{Sp}+} = 3/2$. In the symplectic class with an odd number of channels ($s \ll 1$),

$$\frac{L}{\xi} K_-^{\text{Sp}}(s) = 2 - 4\pi s - ((8s)^2/3) \log(s) + \dots, \quad (18)$$

which signals the presence of a single topologically protected metallic channel, see also Fig 1.

Forward peak:—The form factor deriving from the above results describes the genesis of the forward scattering peak in the quantum quench set-up discussed in the introduction [32, 41],

$$\mathcal{C}_{\text{fs}}^U(t) = \theta(t) I_0(8/t\Delta\xi) e^{-8/t\Delta\xi}, \quad (19)$$

$$\mathcal{C}_{\text{fs}}^O(t) = \theta(t) [I_0(8/t\Delta\xi) + I_1(8/t\Delta\xi)] e^{-8/t\Delta\xi}, \quad (20)$$

$$\mathcal{C}_{\text{fs}}^{\text{Sp},\pm}(t) = \frac{1}{2} [\mathcal{C}_{\text{fs}}^O(t) \pm \theta(t) e^{-4/t\Delta\xi}]. \quad (21)$$

Here we have normalized the peak with respect to its saturation value $\lim_{t \rightarrow \infty} \mathcal{C}_{\text{fs}}(t)$. The forward peak in the unitary class has been calculated previously [14, 43]. Corresponding results for the experimentally relevant orthogonal class [42] and the symplectic class have been unknown. Fig. 2 displays a comparison of our results with recent numerical simulations of the quantum quench experiment in the orthogonal class [43]. The solid line is

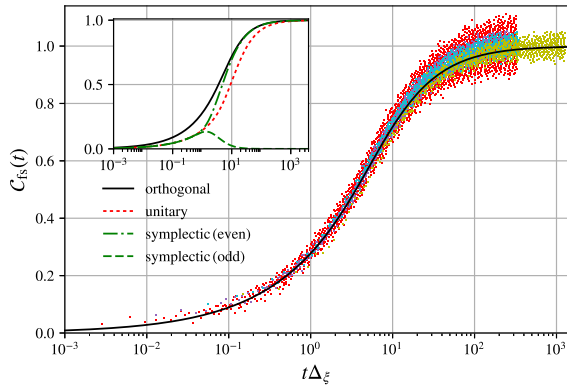


Figure 2: Forward-scattering peak in the orthogonal class. Points are numerical data from a recent simulation of the quantum quench experiment in a kicked rotor set-up [15]. Different colors correspond to different sets of system parameters, and the solid line shows Eq. (20) without any fitting-parameter [44]. Insets: Forward-scattering peak for all Wigner-Dyson classes, see main text for discussion.

Eq. (20) and shows perfect agreement with the numerical data without using any fitting-parameter. The forward peak for all Wigner-Dyson classes are displayed in the inset of Fig. 2. C_{fs}^{O} is readily understood as a sum of diagrams involving only ladders (‘diffuson modes’) C_{fs}^{U} , and diagrams containing crossed ladders (‘Cooperon modes’). $C_{\text{fs}}^{\text{Sp},\pm}$ follows the signal of the unitary class at short times, $\tau \equiv t\Delta_\xi \ll 1$, staying a factor two below the signal in the orthogonal class, and becomes sensitive to the channel number once $\tau \equiv t\Delta_\xi \gtrsim 0.1$. For an odd channel number the signal in the symplectic class then decays to zero as $C_{\text{fs}}^{\text{Sp},-} \sim 4/\tau^2 - 64/(3\tau^3) + \dots$, indicating delocalization due to the presence of the topologically protected channel. Long and short time signals in the remaining cases can be summarized as ($\tau \equiv t\Delta_\xi$)

$$C_{\text{fs}}(\tau) = \begin{cases} a_\alpha \tau^{1/2} + b_\alpha \tau^{3/2} + \dots, & s \ll 1, \\ 1 - c_\alpha/\tau + d_\alpha/\tau^2 + \dots, & s \gg 1, \end{cases} \quad (22)$$

where $a_{\text{O}} = 2a_{\text{U},\text{Sp}+} = 1/(2\sqrt{\pi})$, $b_{\text{O}} = -2b_{\text{U}} = 2b_{\text{Sp}+} = -1/(128\sqrt{\pi})$, $c_{\text{O},\text{Sp}+} = c_{\text{U}}/2 = 4$, and $d_{\text{O}} = d_{\text{U}}/3 = 4d_{\text{Sp}+}/3$.

Local generating function.—The analysis above relied on the representation of the level-level correlation function in terms of a local generating function. The latter derives from the graded symmetry of action (3), which is evident in the polar parametrization $Q = UQ_0U^{-1}$ [10]. Here matrices U are diagonal in ‘ra’-sector and contain all anti-commuting variables, while $Q_0 = \cos \hat{\theta} \sigma_3^{\text{ra}} - \sin \hat{\theta} \sigma_2^{\text{ra}}$ has off-diagonal structure in the latter [32]. The block-diagonal matrices in ‘bf’-sector $\hat{\theta} = \text{diag}(i\hat{\theta}_{\text{b}}, \hat{\theta}_{\text{f}})_{\text{bf}}$, with $\hat{\theta}_{\text{b},\text{f}}$ matrices in ‘tr’-sector, are conveniently parametrized by the non-compact and compact radial variables introduced earlier, $-1 \leq \lambda_{\text{f}} \equiv \cos \theta_{\text{f}} \leq 1$, $1 \leq \lambda_{\text{b}} \equiv$

$\cosh \theta_{\text{b}}$ [10]. The graded symmetry manifests itself in the invariance of action (3) under constant rotations \bar{U} sharing the symmetries of U , $U \mapsto \bar{U}U$. This invariance can be used to linearly shift Grassmann variables in the pre-exponential correlation function, and e.g. implies that finite contributions to the superintegral Eq. (2) may only derive from the maximal polynomial of Grassmann variables $P_{\mathcal{G}}$ [45]. It is then convenient to introduce (unnormalized) maximal polynomials of Grassmann variables in retarded/advanced sectors $P_{\mathcal{G}}^{\text{r/a}}$ with $P_{\mathcal{G}} = P_{\mathcal{G}}^{\text{r}} P_{\mathcal{G}}^{\text{a}}$ and the generating function $\mathcal{F}(\eta, \mathbf{x}) \equiv \left\langle \frac{[\text{str}(k\Lambda Q_\Lambda(\mathbf{x}))]^2}{\text{str}(\Lambda Q(\mathbf{x}))} \right\rangle_S$. Notice that in the quantum-dot limit Q becomes \mathbf{x} -independent, and the generation of Eq. (2) by $\partial_\eta \mathcal{F}$ is immediately evident. For general d -dimensional systems, on the other hand, a straightforward calculation shows that $\mathcal{F}(\eta, \mathbf{x}) = \langle \text{str}(\cos \hat{\theta}_{\mathbf{x}}) P_{\mathcal{G},\mathbf{x}} \rangle_S$ [32, 46], and similarly one finds

$$\partial_\eta \mathcal{F}(\eta, \mathbf{x}) \propto \int (dy) \langle C_{\mathbf{x},\mathbf{y}} P_{\mathcal{G},\mathbf{x}} \rangle_S, \quad (23)$$

$$K(\omega) \propto \int (dx) \int (dy) \langle C_{\mathbf{x},\mathbf{y}} P_{\mathcal{G},\mathbf{x}}^{\text{a}} P_{\mathcal{G},\mathbf{y}}^{\text{r}} \rangle_S, \quad (24)$$

with $C_{\mathbf{x},\mathbf{y}} = \text{str}(\cos \hat{\theta}_{\mathbf{x}}) \text{str}(\cos \hat{\theta}_{\mathbf{y}})$. The graded symmetry can now be used to shift $P_{\mathcal{G},\mathbf{x}(\mathbf{y})}^{\text{r}} \mapsto P_{\mathcal{G},\mathbf{x}}^{\text{r}} + P_{\mathcal{G},\mathbf{y}}^{\text{r}}$, in the first (second) term, which implies that Eq. (2) is generated from the local correlation function for general d -dimensional systems. Indeed, keeping numerical factors one finds $K(\omega) = -(16\pi\tilde{\nu}_0)^{-1} \text{Im} \int (dx) \partial_\omega \mathcal{F}(\omega, \mathbf{x})$, and $\mathcal{F}(\eta) = \frac{8}{\beta} \langle \text{str}(\cos \hat{\theta}_{\mathbf{x}}) P_{\mathcal{G},\mathbf{x}}^{\text{O}} \rangle_S$ with $P_{\mathcal{G}}^{\text{O}}$ now the normalized maximal polynomial of Grassmann variables [32]. Upon integration over the latter one arrives at Eq. (4) for the Anderson insulating wires. Notice that similar ideas have previously been applied in the context of the replicated σ -model [47] and parametric correlations [48]. The representation of level-level correlations in terms of the local generating function may also prove useful in other contexts [49].

Summary.—We have shown that spectral correlations in the Wigner-Dyson classes can be calculated within the supersymmetric σ -model from a local generating function. In Anderson insulating wires this reveals a simple relation between level-level correlations and the ground-state wave-function of the transfermatrix Hamiltonian, which allowed us to derive spectral correlation functions for all Wigner-Dyson classes. The experimental observation of the spectral form factor is within reach of state-of-the-art cold atom quantum quench experiments, and a parameter-free comparison of our findings with recent numerical simulations of the latter shows perfect agreement. The experimental verification of the results reported here would mark an important benchmark for our understanding of strong Anderson localization.

Acknowledgements.—We thank G. Lemarié for providing us with their simulation data of the quantum quench

experiment. T. M. acknowledges financial support by Brazilian agencies CNPq and FAPERJ.

-
- [1] P. W. Anderson, Phys. Rev. **109**, 1492 (1958).
- [2] C. W. Groth, M. Wimmer, A. R. Akhmerov, J. Tworzydło, C. W. J. Beenakker, Phys. Rev. Lett. **103**, 196805 (2009).
- [3] J. Li, R.-L. Chu, J. K. Jain, S.-Q. Shen, Phys. Rev. Lett. **102**, 136806 (2009).
- [4] W. DeGottardi, D. Sen, S. Vishveshwara, Phys. Rev. Lett. **110**, 146404 (2013).
- [5] I. Mondragon-Shem, J. Song, T. L. Hughes, E. Prodan, Phys. Rev. Lett. **113**, 046802 (2014).
- [6] A. Altland, D. Bagrets, A. Kamenev, Phys. Rev. B **91**, 085429 (2015).
- [7] D. Basko, I. Aleiner, B. Altshuler, Ann. Phys. **321**, 1126 (2006).
- [8] I. V. Gornyi, A. D. Mirlin, D. G. Polyakov, Phys. Rev. Lett. **95**, 206603 (2005).
- [9] Strong localization in a driven chaotic system has been observed by J. Chabé, *et al.*, Phys. Rev. Lett. **101**, 255702 (2008). Localization of cold atoms in strictly one-dimensional wave guides has been seen in J. Billy *et al.*, Nature **453**, 891 (2008) and G. Roati *et al.*, Nature **453**, 895 (2008).
- [10] K. B. Efetov, *Supersymmetry in Disorder and Chaos* (Cambridge University Press, 1999).
- [11] T. Karpiuk, N. Cherroret, K. L. Lee, B. Grémaud, C. A. Müller, C. Miniatura, Phys. Rev. Lett. **109**, 190601 (2012).
- [12] K. L. Lee, B. Grémaud, C. Miniatura, Phys. Rev. A **90**, 043605 (2014).
- [13] S. Ghosh, N. Cherroret, B. Grémaud, C. Miniatura, D. Delande, Rev. A **90**, 063602 (2014).
- [14] T. Micklitz, C. A. Müller, A. Altland, Phys. Rev. Lett. **112**, 110602 (2014).
- [15] G. Lemarié, C. A. Müller, D. Guéry-Odelin, C. Miniatura, Phys. Rev. A **95**, 043626 (2017).
- [16] L. P. Gor'kov, G. M. Eliashberg, Zh. Eksp. Teor. Fiz. **48**, 1407 (1965) [Sov. Phys. JETP **21**, 940 (1965)].
- [17] K. B. Efetov, Zh. Eksp. Teor. Fiz. **83**, 833 (1982).
- [18] K. B. Efetov, Adv. Phys. **32**, 53 (1983).
- [19] B. L. Altshuler, B. I. Shklovskii, Zh. Eksp. Teor. Fiz. **91**, 220 (1986) [Sov. Phys. JETP **64**, 127 (1986)].
- [20] B. L. Altshuler, I. Kh. Zharekeshev, S. A. Kotochigova, B. I. Shklovskii, Zh. Eksp. Teor. Fiz. **94**, 343 (1988) [Sov. Phys. JETP **67**, 625 (1988)].
- [21] U. Sivan, Y. Imry, Phys. Rev. B **35**, 6074 (1987).
- [22] I. Kh. Zharekeshev, Fiz. Tverd. Tela (Leningrad) [Sov. Phys. Solid State **31**, 65 (1989)].
- [23] F. M. Izrailev, Phys. Rep. **129**, 299 (1990).
- [24] B. I. Shklovskii, B. Shapiro, H. B. Shore, Phys. Rev. B **47**, 11487 (1992).
- [25] S. N. Evangelou, E. N. Economou, Phys. Rev. Lett. **68**, 361 (1992).
- [26] C. E. Porter, *Statistical Properties of Spectra: Fluctuations*, (Academic, New York, 1965).
- [27] F. Haake, *Quantum Signatures of Chaos*, (Springer, 2010).
- [28] E. Khalaf, P. M. Ostrovsky, arXiv:1707.03369.
- [29] K. B. Efetov, A. Larkin, Sov. Phys. JETP **58**, 444 (1983).
- [30] A. Altland, D. Fuchs, Phys. Rev. Lett. **74**, 4269 (1995).
- [31] The localization length here is always that for the orthogonal class, i.e. $\xi_O = \xi$ while $\xi_U = 2\xi$ and $\xi_{Sp} = 4\xi$.
- [32] See Supplemental Material, where we summarize polar coordinates and zero-modes for the Wigner-Dyson classes, and present details on the local generating function and the calculation of the forward scattering peak.
- [33] T. Micklitz, Phys. Rev. B **93**, 094201 (2016).
- [34] Correcting a factor 4 in Ref. 33.
- [35] M. A. Skvortsov, P. M. Ostrovsky, JETP Lett. **85**, 72 (2007).
- [36] N. F. Mott, Philos. Mag. **22**, 7 (1970).
- [37] U. Sivan, Y. Imry, Phys. Rev. B **35**, 6074 (1987).
- [38] See e.g. D. A. Ivanov, M. A. Skvortsov, P. M. Ostrovsky, Ya. V. Fominov, Phys. Rev. B **85**, 035109 (2012).
- [39] I. S. Gradsteyn and I. M. Ryzhik, *Table of integrals, series, and products* (Academic Press, New York, 2000).
- [40] E. Akkermans, G. Montambaux, *Mesoscopic Physics of Electrons and Photons*, (Cambridge University Press, 2007).
- [41] That is, up to a normalization factor $C_{fs}(t) = \int_{-\infty}^{\infty} d\omega e^{-i\omega t} \partial_{\eta} \mathcal{F}(\eta)$.
- [42] F. Jendrzejewski, K. Müller, J. Richard, A. Date, T. Plisson, P. Bouyer, A. Aspect, V. Josse, Phys. Rev. Lett. **109**, 195302 (2012).
- [43] Notice that here we use $\Delta_{\xi} \equiv \Delta_{\xi}^O = D/\xi_O^2$ with ξ_O the localization length in the orthogonal class, and e.g. $\Delta_{\xi}^U = \Delta_{\xi}^O/4$, see also Ref. 31.
- [44] The universal curve is obtained after accounting for finite Ehrenfest-times and with Heisenberg-times $\sim 1/\Delta_{\xi}$ independently determined from the wave-packet dynamics (see Ref. 15 for further details).
- [45] M. Zirnbauer, Nucl. Phys. B **265**, 375 (1985).
- [46] The pure c -number boundary term here vanishes.
- [47] R. A. Smith, I. V. Lerner, B. L. Altshuler, Phys. Rev. B **58**, 10343 (1998).
- [48] N. Taniguchi, B. D. Simons, B. L. Altshuler, Phys. Rev. B **53**, R7618(R) (1996).
- [49] K. S. Tikhonov, A. D. Mirlin Phys. Rev. B **94**, 184203 (2016).

Supplemental Material to: "Spectral correlations in Anderson insulating wires"

M. Marinho and T. Micklitz

Centro Brasileiro de Pesquisas Físicas, Rua Xavier Sigaud 150, 22290-180, Rio de Janeiro, Brazil

(Dated: July 3, 2021)

In this Supplemental Material, we summarize polar coordinates for Q -matrices and zero-modes of the transfermatrix Hamiltonian in the three Wigner-Dyson classes. We present details on the local generating function, the evaluation of the boundary integrals, and the calculation of the forward scattering peak.

PACS numbers: 72.15.Rn, 73.20.Fz, 03.75.-b, 42.25.Dd

POLAR COORDINATES AND ZERO MODES

For convenience of the reader we summarize polar coordinates and ground-state wave-functions ('zero-modes') for the three Wigner-Dyson classes.

Polar coordinates:—The decomposition $Q = UQ_0U^{-1}$, was introduced in the main text. Here

$$Q_0 = \begin{pmatrix} \cos \hat{\theta} & i \sin \hat{\theta} \\ -i \sin \hat{\theta} & -\cos \hat{\theta} \end{pmatrix}_{\text{ra}}, \quad U = \begin{pmatrix} u & 0 \\ 0 & v \end{pmatrix}_{\text{ra}}, \quad (25)$$

with $\hat{\theta} = \text{diag}(i\hat{\theta}_{\text{bb}}, \hat{\theta}_{\text{ff}})_{\text{bf}}$, and matrices $\hat{\theta}_{\text{bb}, \text{ff}}$ in 'tr'-sector depending on the fundamental symmetries,

$$\hat{\theta}_{\text{bb}} = \begin{pmatrix} \theta_{\text{b}} & 0 \\ 0 & \theta_{\text{b}} \end{pmatrix}_{\text{tr}}, \quad \hat{\theta}_{\text{ff}} = \begin{pmatrix} \theta_{\text{f}} & 0 \\ 0 & \theta_{\text{f}} \end{pmatrix}_{\text{tr}}, \quad (\text{U}) \quad (26)$$

$$\hat{\theta}_{\text{bb}} = \begin{pmatrix} \theta_{\text{b},1} & \theta_{\text{b},2} \\ \theta_{\text{b},2} & \theta_{\text{b},1} \end{pmatrix}_{\text{tr}}, \quad \hat{\theta}_{\text{ff}} = \begin{pmatrix} \theta_{\text{f}} & 0 \\ 0 & \theta_{\text{f}} \end{pmatrix}_{\text{tr}}, \quad (\text{O}) \quad (27)$$

$$\hat{\theta}_{\text{bb}} = \begin{pmatrix} \theta_{\text{b}} & 0 \\ 0 & \theta_{\text{b}} \end{pmatrix}_{\text{tr}}, \quad \hat{\theta}_{\text{ff}} = \begin{pmatrix} \theta_{\text{f},1} & \theta_{\text{f},2} \\ \theta_{\text{f},2} & \theta_{\text{f},1} \end{pmatrix}_{\text{tr}}, \quad (\text{Sp}), \quad (28)$$

where compact and non-compact parameters $0 < \theta_{\text{f}} < \pi$ and $\theta_{\text{b}} > 0$, respectively [1]. In the main text we use radial variables $-1 \leq \lambda_{\text{f}} \equiv \cos \theta_{\text{f}} \leq 1$, $1 \leq \lambda_{\text{b}} \equiv \cosh \theta_{\text{b}}$, and suppress the graded index b, f in favor of

the 'tr'-index, 1, 2. It is convenient to parametrize $U = U_1U_2$, with $U_i = \text{diag}(u_i, v_i)_{\text{ra}}$ and u_1, v_1 containing all Grassmann variables and u_2, v_2 depending only on c -numbers. The latter are of no further relevance for us, and the former can be parametrized as $u_1(\hat{\eta}) = 1 - 2\hat{\eta} + 2\hat{\eta}^2 - 4\hat{\eta}^3 + 6\hat{\eta}^4$ and $v_1(\hat{\kappa}) = 1 - 2\hat{\kappa} + 2\hat{\kappa}^2 - 4\hat{\kappa}^3 + 6\hat{\kappa}^4$, where

$$\hat{\eta} = \begin{pmatrix} 0 & \eta^\dagger \\ -\eta & 0 \end{pmatrix}_{\text{bf}}, \quad \hat{\kappa} = \begin{pmatrix} 0 & i\kappa^\dagger \\ -i\kappa & 0 \end{pmatrix}_{\text{bf}}, \quad (29)$$

with

$$\eta = \begin{pmatrix} \eta_1 & 0 \\ 0 & -\eta_1^* \end{pmatrix}_{\text{tr}}, \quad \kappa = \begin{pmatrix} \kappa_1 & 0 \\ 0 & -\kappa_1^* \end{pmatrix}_{\text{tr}}, \quad (\text{U}) \quad (30)$$

$$\eta = \begin{pmatrix} \eta_1 & \eta_2 \\ -\eta_2^* & -\eta_1^* \end{pmatrix}_{\text{tr}}, \quad \kappa = \begin{pmatrix} \kappa_1 & \kappa_2 \\ -\kappa_2^* & -\kappa_1^* \end{pmatrix}_{\text{tr}}, \quad (\text{O, Sp}). \quad (31)$$

We recall that $(\eta_i^*)^* = -\eta_i$ and similar for κ_i , and notice that $[u_1(\hat{\eta})]^{-1} = u_1(-\hat{\eta})$, and $[v_1(\hat{\kappa})]^{-1} = v_1(-\hat{\kappa})$ [1].

Zero-modes for Wigner-Dyson classes:—The ground-state wave-functions for the transfermatrix Hamiltonian of the Wigner-Dyson symmetry classes, recently derived in Ref. 2, read ($p = \sqrt{(\lambda + 1)/2}$)

$$Y_0^{\text{U}}(\lambda_{\text{b}}, \lambda_{\text{f}}) = 4\sqrt{\eta} \left(p_{\text{f}} K_0(4\sqrt{\eta} p_{\text{b}}) I_1(4\sqrt{\eta} p_{\text{f}}) + p_{\text{b}} K_1(4\sqrt{\eta} p_{\text{b}}) I_0(4\sqrt{\eta} p_{\text{f}}) \right), \quad (32)$$

$$Y_0^{\text{O}}(\lambda_1, \lambda_2, \lambda_{\text{f}}) = \sqrt{\eta} \left(4p_1 p_2 I_0(4\sqrt{\eta} p_{\text{f}}) K_1(4\sqrt{\eta} p_1 p_2) + \frac{1}{p_{\text{f}}} (1 + \lambda_1 + \lambda_2 + \lambda_{\text{f}}) I_1(4\sqrt{\eta} p_{\text{f}}) K_0(4\sqrt{\eta} p_1 p_2) \right), \quad (33)$$

$$Y_0^{\text{Sp}}(\lambda_{\text{b}}, \lambda_1, \lambda_2) = \sqrt{\eta} \left(4p_1 p_2 I_1(4\sqrt{\eta} p_1 p_2) K_0(4\sqrt{\eta} p_{\text{b}}) + \frac{1}{p_{\text{b}}} (1 + \lambda_1 + \lambda_2 + \lambda_{\text{b}}) I_0(4\sqrt{\eta} p_1 p_2) K_1(4\sqrt{\eta} p_{\text{b}}) \right), \quad (34)$$

$$Y_{\pm}^{\text{Sp}}(\lambda_{\text{b}}, \lambda_1, \lambda_2) = Y_0^{\text{Sp}}(\lambda_{\text{b}}, \lambda_1, \lambda_2) \pm Y_0^{\text{Sp}}(\lambda_{\text{b}}, -\lambda_1, -\lambda_2). \quad (35)$$

GENERATING FUNCTION

Starting out from the generating function, introduced in the main text,

$$\mathcal{F}(\eta, \mathbf{x}) = \left\langle \frac{[\text{str}(k\Lambda Q_{\Lambda}(\mathbf{x}))]^2}{\text{str}(\Lambda Q(\mathbf{x}))} \right\rangle_S, \quad (36)$$

it is verified that in polar coordinates

$$\text{str}(\Lambda Q) = 2 \text{str}(\cos \hat{\theta}), \quad (37)$$

$$\text{str}(k\Lambda Q) = \text{str}(k\Lambda U_2^{-1} U_1^2 U_2 Q_0), \quad (38)$$

where in the second line we employed cyclic invariance of the trace and anti-commutation of $\hat{\eta}$ and k . $kU_2^{-1}U_1^2U_2$ is a diagonal matrix in ‘ra’-sector, with ‘rr’-block

$$\begin{aligned} & [kU_2^{-1}U_1^2U_2]_{\text{rr}} \\ &= u_2^{-1}k \left[1 - 8 \begin{pmatrix} \eta^\dagger \eta^{-4}(\eta^\dagger \eta)^2 & 0 \\ 0 & \eta \eta^\dagger - 4(\eta \eta^\dagger)^2 \end{pmatrix}_{\text{bf}} \right] u_2 + \dots \end{aligned} \quad (39)$$

The omitted terms ‘...’ summarize contributions off-diagonal in ‘bf’-sector, i.e. vanishing under the trace. A similar expression involving κ holds for the ‘aa’-block.

In the unitary class η is diagonal in the ‘tr’-sector, i.e. $\eta^\dagger \eta = -\eta \eta^\dagger = \eta_1^* \eta_1 \mathbb{1}_{\text{tr}}$, and $(\eta^\dagger \eta)^2 = 0$. In the remaining classes η has off-diagonal structure in the ‘tr’-sector and $(\eta^\dagger \eta)^2 = -(\eta \eta^\dagger)^2 = 2\eta_1^* \eta_2^* \eta_1 \eta_2 \mathbb{1}_{\text{tr}}$. Recalling that in any correlation function we only need to account for contributions independent of Grassmann variables or being of maximal order of the latter (see e.g. Ref. 3) we may simplify

$$[kU_2^{-1}U_1^2U_2]_{\text{rr}} = k - \mathcal{P}_{\mathcal{G}}^r + \dots, \quad (40)$$

with $\mathcal{P}_{\mathcal{G}}^r \propto \eta_1^* \eta_1$ and $\mathcal{P}_{\mathcal{G}}^r \propto \eta_1^* \eta_2^* \eta_1 \eta_2$ the (unnormalized)

maximal polynomials of Grassmann variables in the retarded sector for the unitary, respectively, the orthogonal and symplectic symmetry classes. A similar calculation for the ‘aa’-block then leads to

$$\text{str}(k\Lambda Q) = \text{str}([2k + P_{\mathcal{G}}^r + P_{\mathcal{G}}^a] \cos \hat{\theta}) + \dots, \quad (41)$$

where omitted contributions ‘...’ give again vanishing contributions to the correlation function. That is, keeping only terms with non-vanishing contributions to the correlation function,

$$[\text{str}(k\Lambda Q_\Lambda)]^2 = [\text{str}(2k(\cos \hat{\theta} - \mathbb{1}_4))]^2 + 2[\text{str}(\cos \hat{\theta})]^2 P_{\mathcal{G}}, \quad (42)$$

with $P_{\mathcal{G}} = P_{\mathcal{G}}^r P_{\mathcal{G}}^a$ the (unnormalized) maximal polynomial in Grassmann variables. Similarly,

$$\mathcal{F}(\eta, \mathbf{x}) = \left\langle \text{str}(\cos \hat{\theta}) P_{\mathcal{G}} \right\rangle_S, \quad (43)$$

where we noticed that boundary terms (i.e. those independent of Grassmann variables) here vanish. Finally,

$$\int (dx) \int (dy) \langle \mathcal{F}(\eta, \mathbf{x}) \text{str}(\Lambda Q(\mathbf{y})) \rangle_S = 2 \int (dx) \int (dy) \langle \text{str}(\cos \hat{\theta}(\mathbf{x})) \text{str}(\cos \hat{\theta}(\mathbf{y})) P_{\mathcal{G}}(\mathbf{x}) \rangle_S, \quad (44)$$

$$\int (dx) \int (dy) \langle \text{str}(k\Lambda Q_\Lambda(\mathbf{x})) \text{str}(k\Lambda Q_\Lambda(\mathbf{y})) \rangle_S = 2 \int (dx) \int (dy) \langle \text{str}(\cos \hat{\theta}(\mathbf{x})) \text{str}(\cos \hat{\theta}(\mathbf{y})) P_{\mathcal{G}}^a(\mathbf{x}) P_{\mathcal{G}}^r(\mathbf{y}) \rangle_S, \quad (45)$$

and both expression become identical upon shifting $P_{\mathcal{G}}^r(\mathbf{x}) \mapsto P_{\mathcal{G}}^r(\mathbf{x}) + P_{\mathcal{G}}^r(\mathbf{y})$, in the first term, and $P_{\mathcal{G}}^r(\mathbf{y}) \mapsto P_{\mathcal{G}}^r(\mathbf{y}) + P_{\mathcal{G}}^r(\mathbf{x})$ in the second term, as discussed in the main text. To fix all factors, we can then normalize the maximal polynomial of Grassmann variables by considering the quantum-dot limit, where $Q(\mathbf{x}) = Q_0$ is space-independent. That is, for

$$P_{\mathcal{G}} = \frac{8}{\beta} P_{\mathcal{G}}^0, \quad (46)$$

with $P_{\mathcal{G}}^0$ the normalized maximal polynomial of Grassmann variables (introduced in the main text) Eq. (43) recovers Wigner-Dyson statistics [4].

BOUNDARY TERMS

In the main text we have derived the following representation for the generating function for level-level correlations in one of the three Wigner-Dyson classes,

$$\mathcal{F}(\eta) = \int d\mathcal{R} \partial_\lambda \sqrt{g} g^{\lambda\rho} (Y'_0 \partial_\rho Y_0 - Y_0 \partial_\rho Y'_0), \quad (47)$$

where $Y'_0 \equiv \partial_\eta Y_0$. We next discuss different ways to regularize Eq. (47), all leading to the same result.

Unitary class:—Calculations are the simplest in the unitary class, where Eq. (47) takes the form

$$\mathcal{F}^U(\eta) = \int_1^\infty d\lambda_b \int_{-1}^1 d\lambda_f \left(\partial_{\lambda_f} \frac{(1 - \lambda_f^2) G_f(\lambda_b, \lambda_f)}{(\lambda_b - \lambda_f)^2} + \partial_{\lambda_b} \frac{(\lambda_b^2 - 1) G_b(\lambda_b, \lambda_f)}{(\lambda_b - \lambda_f)^2} \right), \quad (48)$$

and to simplify notation we introduced $G_{f,b} \equiv Y'_0 \partial_{\lambda_{f,b}} Y_0 - Y_0 \partial_{\lambda_{f,b}} Y'_0$. As discussed in the main text, the

first (second) term vanishes at the boundary $\lambda_f = 1$ ($\lambda_b =$

1). At the same time the Jacobian $\sqrt{g} = 1/(\lambda_b - \lambda_f)^2$ diverges at $\lambda_f = \lambda_b = 1$. To deal with this situation we regularize (some of) the radial variables shifting the limit of integration $1 \mapsto 1^\pm \equiv 1 \pm \epsilon$, where the positive/negative sign applies for the bosonic/fermionic radial variable. Regularizing e.g. in the bosonic radial variable,

$$\mathcal{F}^U(\eta) = 2 \lim_{\epsilon \rightarrow 0} \int_0^\infty dx_f \frac{\epsilon G_f(1, 1)}{(x_f + \epsilon)^2} = 2G_f(1, 1), \quad (49)$$

where $x_f = 1 - \lambda_f$ and we used that in the limit $\epsilon \searrow 0$ we only need to keep leading contributions in $x_f \ll 1$. Similarly, one finds upon regularization in the fermionic radial variable $\mathcal{F}^U(\eta) = -2G_b(1, 1)$. If, on the other hand, both variables are regularized,

$$\begin{aligned} \mathcal{F}^U(\eta) &= 2 \lim_{\epsilon \rightarrow 0} \left(\int_\epsilon^\infty dx_f \frac{\epsilon G_f(1, 1)}{(x_f + \epsilon)^2} - \int_\epsilon^\infty dx_f \frac{\epsilon G_b(1, 1)}{(x_f + \epsilon)^2} \right) \\ &= G_f(1, 1) - G_b(1, 1), \end{aligned} \quad (50)$$

and the same is found in polar coordi-

nates upon excluding $r = 0$, i.e. $\mathcal{F}^U(\eta) = 2 \lim_{\epsilon \rightarrow 0} \int_0^{\pi/2} d\phi \left(\frac{\cos^2 \phi G_f(1, 1)}{(\cos \phi + \sin \phi)^2} - \frac{\sin^2 \phi G_b(1, 1)}{(\cos \phi + \sin \phi)^2} \right)$. Noting that $G_f(1, 1) = -G_b(1, 1)$ it is verified that all of the above procedures give the same result.

Other classes:—Calculations in the orthogonal and symplectic classes are more involved but follow the same line. Upon regularization, the boundary contribution $(\sqrt{g}g^{\lambda\rho})|_{\lambda=1^\pm}$ in Eq. (47) reduces (up to a numerical factor) to a δ -function in the remaining radial coordinates, fixing the latter to $\lambda = 1$. Zero-modes in all symmetry classes share the properties that $Y_0(\Lambda) = 1$, $Y'_0(\Lambda) = 0$, and $\partial_\lambda Y'_0|_{Q=\Lambda} = \pm \partial_\rho Y'_0|_{Q=\Lambda}$. Here the positive sign applies if λ and ρ are both bosonic or fermionic radial variables and the negative sign else, and we recall that Λ corresponds to setting all radial variables $\lambda = 1$. These properties guarantee that the result is independent of which/how many integration limits are shifted.

Changing e.g. in the orthogonal class the integration limit in the fermionic variable,

$$\begin{aligned} \mathcal{F}^O(\eta) &= \lim_{\epsilon \rightarrow 0} \int_1^\infty d\lambda_1 \int_1^\infty d\lambda_2 \int_{-1}^{1-\epsilon} d\lambda_f \partial_{\lambda_f} \sqrt{g} g^{\lambda_f \lambda_f} G_f(\lambda_f, \lambda_1, \lambda_2) \\ &= \lim_{\epsilon \rightarrow 0} \int_1^\infty d\lambda_1 \int_1^\infty d\lambda_2 \frac{4\epsilon^2 G_f(1, \lambda_1, \lambda_2)}{(\epsilon^2 + \lambda_1^2 + \lambda_2^2 - 2\lambda_1\lambda_2 - 2\epsilon(1 - \lambda_1\lambda_2))^2} = 2G_f(1, 1, 1), \end{aligned} \quad (51)$$

while a similar calculation with any of the two integration limits $\lambda_{1,2}$ shifted gives $\mathcal{F}^O(\eta) = -2G_b(1, 1, 1)$, etc. As stated in the main text, we may, therefore, equivalently present the final results in a symmetrized form, e.g.

$$\mathcal{F}_0^U(\eta) = (\partial_{\lambda_b} - \partial_{\lambda_f}) Y'_0|_{\lambda_b=\lambda_f=1}, \quad (52)$$

in the unitary class, and similarly for the other symmetry classes.

FORWARD PEAK

The time evolution of the forward scattering peak is, up to a normalization factor, given by the Fourier transform of the level-level correlation function. E.g. in the

unitary class ($\eta = -i\omega/\Delta_\xi$)

$$\begin{aligned} \mathcal{C}_{\text{fs}}(t) &\propto \Delta_\xi^{-1} \int_{-\infty}^\infty d\omega e^{-i\omega t} \partial_\eta K_0(4\sqrt{\eta}) I_0(4\sqrt{\eta}) \\ &= i\Delta_\xi t \theta(t) \int_0^\infty dz e^{-zt\Delta_\xi} \left(K_0(4i\sqrt{z}) I_0(4i\sqrt{z}) \right. \\ &\quad \left. - K_0(-4i\sqrt{z}) I_0(-4i\sqrt{z}) \right) \\ &= \Delta_\xi t \theta(t) \int_0^\infty dz e^{-zt\Delta_\xi} J_0(4\sqrt{z}) J_0(4\sqrt{z}) \\ &= \theta(t) I_0 \left(\frac{8}{\Delta_\xi t} \right) e^{-\frac{8}{\Delta_\xi t}}, \end{aligned} \quad (53)$$

where in the third line we used that $K_n(-z) = (-1)^n K_n(z) + (\log(z) - \log(-z)) I_n(z)$, $I_n(-z) = (-1)^n I_n(z)$, and $I_n(iz) = i^n J_n(z)$. A similar calculation for the remaining classes, leads to Eqs. (19)-(21) stated in the main text.

[1] K. B. Efetov, *Supersymmetry in Disorder and Chaos* (Cambridge University Press, 1999).

- [2] E. Khalaf, P. M. Ostrovsky, arXiv:1707.03369.
- [3] M. Zirnbauer, Nucl. Phys. B **265**, 375 (1985).
- [4] Notice that we here used that integrals over variables

parametrizing U_2 are normalized.